Drag Forces in a Coupled Wave Ice Model: Implementation and Testing

- Mark Orzech[1]*, Fengyan Shi[2], and Jay Veeramony[1]
- [1] NRL Oceanography Division, Stennis Space Center, MS 39529
- [2] CACR, University of Delaware, Newark, DE 19716
- * Email: mark.orzech@nrlssc.navy.mil

Summary:

We are developing a system for modeling the interactions between ocean surface waves and polar ice floes, which consists of a nonhydrostatic, finite-volume wave model (NHWAVE) coupled to a discrete element, particle-tracking ice model (LIGGGHTS). The effects of drag forces between fluid and ice were recently implemented in the coupled system. The drag formulations assume that the fluid velocity profile at the interface is logarithmic, leading to a drag coefficient that is a function of both grid size and a configurable roughness height. Net forcing vectors acting on the ice in each fluid cell are computed in the wave model and passed to the ice model at each time step. The vectors combine forces due to drag with additional forces due to dynamic pressure (buoyancy effects are computed separately in LIGGGHTS). This presentation provides further details on these new features and summarize the results of several tests conducted to validate them.

Coupled System Overview

The coupled wave-ice system consists of two linked models: a non-hydrostatic, fully dispersive surface wave model (NHWAVE) and a particle-tracking code that represents ice floes as collections of bonded discrete elements (LIGGGHTS). Relevant physical data are passed between the two model domains via the integrated coupling software.

NHWAVE utilizes a modified Cartesian grid in which the vertical z-coordinate has been transformed to a surface- and bed-following sigma-coordinate. The effects of a given ice floe on the fluid are represented using surface boundary conditions, mapping the shape of the underside of each floe onto an upper sigma-level slightly below the surface using 3D masks that move with the floe. An immersed boundary method is used along the floe sides to determine the lateral effects on the fluid. Fluid fluxes and pressure variations are computed from the accelerations at floe/cell boundaries. The vertical velocity of the fluid along the underside of the floe is determined from the kinematic boundary condition at the floe's bottom boundary.

LIGGGHTS initially creates ice floes by defining bonding forces that act within a random close packing of spherical elements. A Voronoi tesselation technique is then employed to delineate more variable element shapes and compute volume, mass, and density. Inter-element forces are assumed to be elastic, with a linear constant of proportionality. Critical fracture stresses are specified so that ice floes may both deform and break in response to wave-generated stresses. The ice floe equation of motion includes internal contact and bond forces as well as external forces from gravity, buoyancy, fluid pressure gradients, and drag.

Coupling software for the (Fortran-based) NHWAVE and (C++-based) LIGGGHTS models was developed within the LIGGGHTS framework. The primary subroutines were written in C++, and each was paired with a corresponding Fortran header to facilitate access by NHWAVE. To jointly compile the separate wave and ice models, the complete LIGGGHTS code, including the coupling subroutines, is first compiled in C++ as a shareable library. The library, along with the coupling header files, is incorporated into the Fortran compilation of NHWAVE. The final executable program can then access all necessary DEM utilities and call on LIGGGHTS to perform ice-related computations as needed.

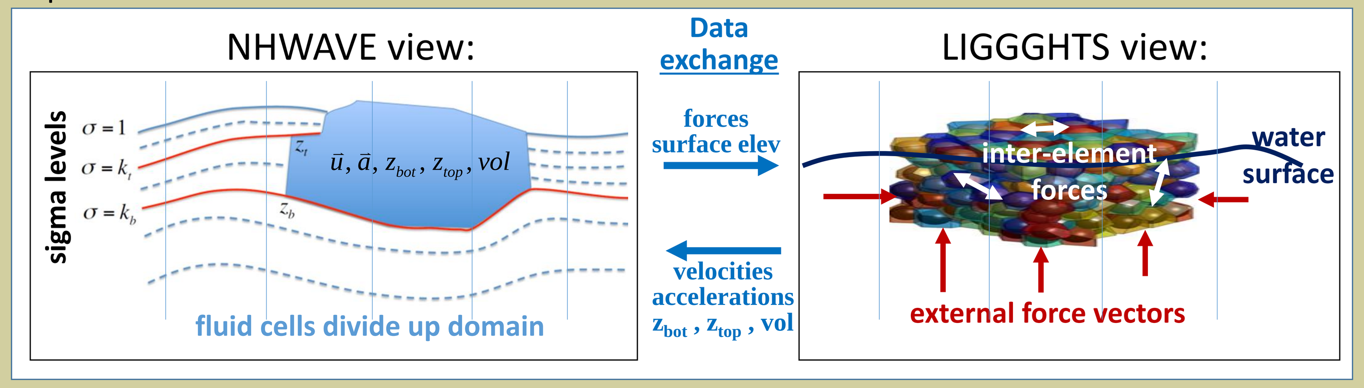

The diagram above illustrates the wave-ice environment as viewed by each of the two models and the data that are exchanged between the two models. While NHWAVE sees a solid block surrounded by oscillating sigma layers, LIGGGHTS sees a collection of bonded elements subjected to both external and internal forces. Information that is passed from waves to ice includes the fluid forces on the ice, the surface elevation in each cell, and (at the first time step) the number and dimensions of the fixed fluid cells. Information passed from ice to waves includes elevations of the highest (**z_{top}**) and lowest (**z_{bot}**) ice elements, average velocities, average accelerations, and total volume of the ice elements in each fluid cell (***vol***). In the wave model, an ice block is considered to occupy all contiguous fluid cells for which ***vol*** is greater than half of the total cell volume between **z_{bot}** and **z_{top}**.

Drag Force Implementation

Extending the implementation of fluid-object interaction described above (and in further detail in Orzech et al., 2016), formulations for the drag force have now been incorporated into the coupled model system. In general, the motion of an ice floe follows but does not exactly match that of the surrounding fluid when there are waves. The velocity shear between the floe and the water produces drag forces that act on both the fluid and the ice. Computation of the ice-fluid drag force has been implemented in the wave model, based on the assumption that the velocity profile at the interface follows the distribution of a stably stratified logarithmic boundary layer. Consequently, the drag coefficient, C_d, may be expressed as

$$C_d = \left(\frac{\kappa}{\ln(30\Delta z/K_s)}\right)^2$$

where κ=0.41 is the von Karmann constant, Δz is vertical grid spacing and K_s is roughness height that can be specified by the user (values ranging from 1mm – 50cm were used here). The dynamic boundary conditions at the wave-ice interfaces in the x-z plane, y-z plane, and x-y plane, respectively, are written as

$$\mu_t \frac{\partial u}{\partial y} = C_d\left|\vec{u}-\vec{u}_{obs}\right|(u-u_{obs}), \qquad \mu_t \frac{\partial w}{\partial y} = C_d\left|\vec{u}-\vec{u}_{obs}\right|(w-w_{obs})$$

$$\mu_t \frac{\partial v}{\partial x} = C_d\left|\vec{u}-\vec{u}_{obs}\right|(v-v_{obs}), \qquad \mu_t \frac{\partial w}{\partial x} = C_d\left|\vec{u}-\vec{u}_{obs}\right|(w-w_{obs})$$

$$\mu_t \frac{\partial u}{\partial z} = C_d\left|\vec{u}-\vec{u}_{obs}\right|(u-u_{obs}), \qquad \mu_t \frac{\partial v}{\partial y} = C_d\left|\vec{u}-\vec{u}_{obs}\right|(v-v_{obs})$$

where μ_t is the dynamic viscosity, $\vec{u}$ and $\vec{u}_{obs}$ represent the fluid velocity and the object velocity, respectively, and *u*, *v*, and *w* are components of these velocities in the *x*, *y*, and *z* directions, respectively.

These equations are solved numerically in NHWAVE using forward and backward differences and result in modified fluid fluxes along the edges of the floating objects. For example, for the ice floe cell at location (*i, j, k*), next to the fluid cell at location (*i, j-1, k*), the horizontal and vertical fluid velocities in the ice floe "ghost" cell are obtained from

$$u(i,j,k) = (1-\phi)u(i,j-1,k) + u_{obs}$$
$$w(i,j,k) = (1-\phi)w(i,j-1,k) + w_{obs}$$

where

$$\phi = C_d\left|\vec{u}-\vec{u}_{obs}\right| / \mu_t$$

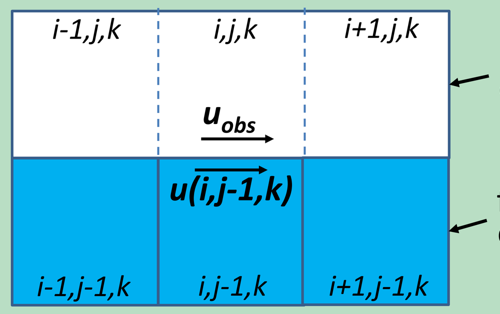

Results of these computations are also used to compute drag forces acting on the ice floes, which are then passed to LIGGGHTS.

Testing of Drag Force

Initial testing of drag force effects utilized a 10m x 10m x 1m ice block, displaced by 20cm from its equilibrium position and then released. In each simulation, the ice block was allowed to "bounce" in the water until its motion was largely damped out.

The mean bouncing block elevation was measured in three separate simulations. Block roughness K_s was set to either 1mm or 50cm, and the model's eddy viscosity parameter μ was concurrently set either to 0.01 m^2/s or 0.30 m^2/s. The figure at right displays the vertical position versus time for the oscillating block, with the legend detailing the settings for each different configuration.

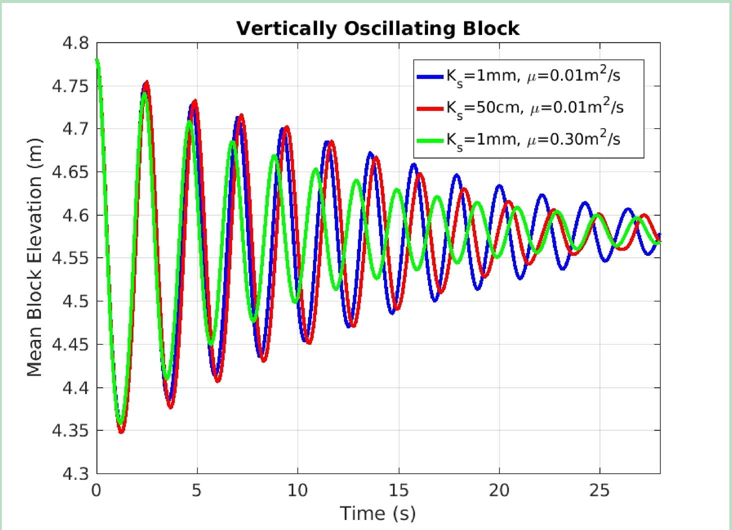

As expected, the oscillations are more rapidly damped for ice floes with greater surface roughness or fluid with greater viscosity. To quantify the result, we use a damping coefficient, K_{damp}, expressed as

$$K_{damp} = A_{n+1}/A_n$$

where A_i represents the oscillation amplitude for cycle number *i*. For the above three cases (blue, red, green lines, respectively), we find that average K_{damp} = 0.84, 0.82, and 0.81. It should also be noted that the different roughness and viscosity settings affect the period of the oscillations, with the fastest oscillations occurring in the high viscosity (green) case and the slowest oscillations occurring in the original (low roughness, low viscosity, blue) case.

General System Performance: Ice Block in Waves

The behavior of the wave-ice system under more typical conditions was tested by simulating the motion of an ice floe in monochromatic waves. With roughness height set to 1cm and viscosity to 0.10 m^2/s, a 10m x 10m x 1m ice floe was positioned at x≈205m in a flume, roughly 100m in front of a wavemaker. As waves with height of 50cm and period of 5sec propagated from the wavemaker and past the ice block, the model recorded the block position and orientation along with the surface elevation and the fluid pressure and velocity fields.

From a close-up side view of the fluid region surrounding the block in a wave trough at t=46sec (below), we find the behavior of the wave-ice system to be generally realistic. The fluid fluxes (arrows) under the leading edge of the block have intensified and become nearly horizontal as they must avoid the dipping corner of the ice. (NB: The velocity magnitudes themselves actually decrease gradually from a maximum of 27cm/s at x=205m to 19cm/s at x=202m, suggesting that some energy may have been lost due to wave-ice shear.)

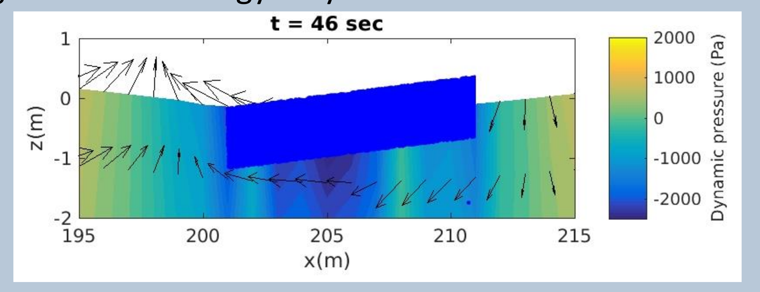

When the mean vertical position of the ice block over time is plotted along with the water surface elevation at x=205m (below), it is possible to see the lag in the ice oscillations (dashed line) relative to those of the waves (solid line).

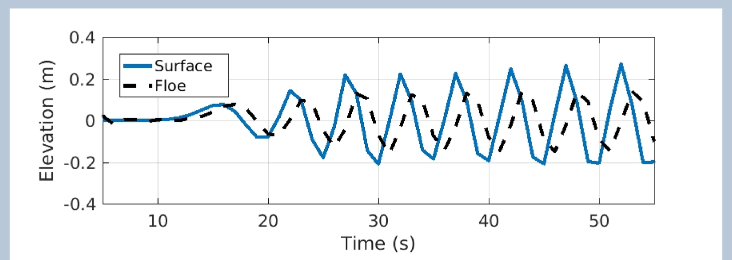

In this case, the vertical motion of the ice floe lags the free surface by approximately 1sec, or one-fifth of a wave period. This lag corresponds to the response time required for the floe to alter its motion as the buoyancy and drag forces change and is a typical characteristic of floating objects in shorter-period wind waves.

Conclusions and Future Plans

The results presented here demonstrate that the coupled wave-ice system can realistically simulate the effects of drag on a floating object in still water or waves. When object roughness is increased, the oscillatory motion of a "bouncing" ice floe is more rapidly damped. Similarly, when fluid viscosity is increased, a greater rate of attenuation is observed in the vertical oscillations. In response to the propagation of monochromatic waves, the vertical motion of the test floe is similar to that of the waves but lags somewhat behind it, as would be expected. These conclusions remain qualitative, however, as comparative laboratory experiments were not conducted.

In the near future, coupled system performance will be more quantitatively validated, via comparison with published experimental and field data. Then system will be applied to a range of scenarios designed to investigate momentum and energy balances in the marginal ice zone. In these "virtual experiments", we will vary the size distribution, material strength, and dimensions of ice floes along with the amplitude, frequency and direction of the waves. Total energy and momentum will be tracked throughout the system, and the processes most responsible for wave attenuation and ice fracturing will be identified.

The long term goal of this project is to develop a tool for evaluating and validating large-scale parameterizations of wave attenuation by ice floes, which will help to improve representations of regional and basin-scale models like NRL's Arctic Cap system (ACNFS).

Acknowledgments

This project is supported by base funding to the Naval Research Lab provided by the Office of Naval Research, and by ONR Award #N00014-14-1-0569. Much of the computational work was accomplished using a grant of supercomputer time from the Department of Defense High Performance Computing Modernization Program (HPCMP) as part of subproject #06632054.

A11D - 1924